arXiv:2204.00070v3 [cond-mat.stat-mech] 13 Sep 2022

KPZ physics and phase transition in a classical single random walker under continuous measurement

Tony Jin[1,*] and David G. Martin[2,†]

[1] *DQMP, University of Geneva, 24 Quai Ernest-Ansermet, CH-1211 Geneva, Switzerland*
[2] *Enrico Fermi Institute, The University of Chicago, 933 E 56th St, Chicago, Illinois 60637, USA*

We introduce and study a new model consisting of a single classical random walker undergoing continuous monitoring at rate γ on a discrete lattice. Although such a continuous measurement cannot affect physical observables, it has a non-trivial effect on the probability distribution of the random walker. At small γ, we show analytically that the time-evolution of the latter can be mapped to the Stochastic Heat Equation (SHE). In this limit, the width of the log probability thus follows a Family-Vicsek scaling law, $N^{\alpha} f(t/N^{\alpha/\beta})$, with roughness and growth exponents corresponding to the Kardar-Parisi-Zhang (KPZ) universality class, i.e $\alpha^{\rm 1D}_{\rm KPZ} = 1/2$ and $\beta^{\rm 1D}_{\rm KPZ} = 1/3$ respectively. When γ is increased outside this regime, we find numerically in 1D a crossover from the KPZ class to a new universality class characterized by exponents $\alpha^{\rm 1D}_{\rm M} \approx 1$ and $\beta^{\rm 1D}_{\rm M} \approx 1.4$. In 3D, varying γ beyond a critical value $\gamma^{c}_{\rm M}$ leads to a phase transition from a smooth phase that we identify as the Edwards-Wilkinson (EW) class to a new universality class with $\alpha^{\rm 3D}_{\rm M} \approx 1$.

Universality is a pillar concept of statistical physics, classical and quantum alike. The fact that, under renormalization, different microscopic models can lead to the same scale invariant theory has been the key idea for understanding second-order phase transitions. In particular, the concept of universality classes has found an extremely fertile ground within the study of dynamical interfaces for which a scale invariance property has been reported and documented [1, 2]. In this context, one particular fixed point has attracted a tremendous interest in the previous decades: the Kardar-Parisi-Zhang (KPZ) universality class and its iconic 1/3 growth exponent [3, 4] in 1D. Beyond the eponym KPZ equation, it has been found in a variety of models describing growing interfaces such as the ballistic deposition model [5], the Eden model [6, 7], or the restricted solid-on-solid model [8]. Perhaps more surprisingly, in the recent years, it has also been discovered in a variety of quantum phenomena such as the growth of entanglement entropy in random unitary circuits [9], stochastic conformal field theory [10], noisy fermions [11] and transport properties of dipolar spin ensembles [12] and integrable spin chains [13–16].

Continuous or weak measurement has enjoyed considerable interest in the previous decades within the quantum community as it provides a non-destructive way to obtain information about a given quantum system [17, 18]. Its advent led to many interesting applications such as quantum Zeno effects [19], quantum trajectories [20], quantum Maxwell demons [21], or direct observation of quantum jumps [22]. Recently, a number of studies investigated the consequences of repeated projections or continuous monitoring on the evolution of quantum many-body systems. For systems undergoing both a random unitary evolution and measurements, a result that has aroused considerable interests lately is the existence of a Measurement-Induced Phase Transition (MIPT) in the entanglement entropy [23–35]. Most of these contributions focus on entanglement or Rényi entropies, i.e information-related quantities which are likely salients in classical systems as well. As such, it is natural to wonder whether the same phenomenology of MIPT also features in classical physics.

In this paper we unveil a connection between KPZ physics and *classical* information theory by studying a single classical random walker undergoing continuous monitoring and, relying on this connection, we show that this system presents a MIPT in 3D.

We first present the framework that we use to model weak, continuous measurements on a generic Markov process. We then focus on the specific case of a single random walker diffusing on a lattice with the occupancy at each site being continuously monitored.

When the measurement rate γ is small, we find in 1D that the standard deviation of the log probability follows a Family-Vicsek scaling law with roughness and growth exponents corresponding to the KPZ universality class, i.e $\alpha^{\rm 1D}_{\rm KPZ} = 1/2$ and $\beta^{\rm 1D}_{\rm KPZ} = 1/3$ respectively [3]. By performing a perturbative analysis around $\gamma = 0$, we show analytically that this KPZ-like behavior is due to a direct mapping of the dynamics onto the Stochastic Heat Equation (SHE). As γ is increased further, we see numerically in 1D a size-dependent crossover between the KPZ regime and a new universality class characterized by different exponents $\alpha^{\rm 1D}_{\rm M} \approx 1$ and $\beta^{\rm 1D}_{\rm M} \approx 1.4$. In 3D, instead of a crossover, we see a phase transition between a smooth phase that we identify as the EW class and a rough phase with $\alpha^{\rm 3D}_{\rm M} \approx 1$. We also show that, both in 1D and 3D, the small γ limit can alternatively be thought as a short time limit $t \ll \gamma^{-1}$ within which the dynamics is described by the KPZ equation.

Continuous monitoring We begin by introducing the formalism of continuous monitoring. It is directly inspired from weak measurement and trajectory frameworks of quantum mechanics [17, 36–39] and can be thought as a simple hidden Markov process [40].

In the absence of monitoring, the system undergoes

a stochastic dynamics generated by $\mathcal{L}$ on a classical configuration space $\mathcal{M}(\mathcal{C})$ with total number of configurations Ω. The time-evolution of the probability distribution $\mathcal{P}_t$ is given by the master equation

$$\frac{d}{dt}\mathcal{P}_t(\mathcal{C}) = \mathcal{L}(\mathcal{P}_t(\mathcal{C})). \tag{1}$$

We assume that the stationary state is unique and is further given by the maximally entropic state $\mathcal{P}_\infty = \Omega^{-1}$. Weak monitoring takes place via an ancilla that couples to the system for a short amount of time δt such that the generated correlation is of order δt as well. Measuring the ancilla's state provides indirect and noisy information about the system which can be used to write a constrained stochastic evolution for $\mathcal{P}_t$.

Let Ω be the set $\{X_1, \cdots, X_N\} := \vec{X}$ where the X_j's can take values ± 1: $+1$ corresponds to an occupied site while -1 to an empty one. We suppose that all sites will be independently monitored. The ancilla monitoring site j is also described by a random variable A_j which can take binary values $a_j \in \{-1, 1\}$. We denote by $\mathcal{P}(\vec{X}, A_j)$ the joint probability of the union system+ancillae to be in a given configuration. We fix this probability distribution to positively correlate the state of the system and of the ancilla :

$$\mathcal{P}(\vec{X}, A_j) = \mathcal{P}(\vec{X})\frac{1 + \frac{\sqrt{\gamma\delta t}}{2}A_j X_j}{2} , \tag{2}$$

where $\mathcal{P}(\vec{X})$ is the reduced probability of the system only. Once a measurement of the ancilla's state has been made with outcome a_j, the probability distribution is updated with probability $1 + \frac{\sqrt{\gamma\delta t}}{2}a_j\langle X_j\rangle$ to

$$\mathcal{P}(\vec{X}) \to \mathcal{P}(\vec{X}|A_j = a_j) = \mathcal{P}(\vec{X})\frac{1 + \frac{\sqrt{\gamma\delta t}}{2}a_j X_j}{1 + \frac{\sqrt{\gamma\delta t}}{2}a_j\langle X_j\rangle}, \tag{3}$$

where $\langle X_j\rangle := \sum_{\{\vec{X}\}} X_j \mathcal{P}_t(\vec{X})$. In the SM [41], we show that repeating this procedure M times and taking the limit $M \to \infty$, $\delta t \to 0$ while keeping $M\delta t = t$ fixed leads, in the Itō prescription, to the following evolution for the probability distribution

$$d\mathcal{P}_t(\vec{X}) = \frac{\sqrt{\gamma}}{2}\mathcal{P}_t(\vec{X})(X_j - \langle X_j\rangle_t)dB_t^j , \tag{4}$$

where dB_t^j are site-independent Brownian processes with variance dt and Itō rules $dB_t^j dB_t^k = \delta_{j,k}dt$. Note that $\mathcal{P}_t$ is both a probability distribution and a stochastic variable. Consequently, there are two types of averages in the problem: $\langle\rangle$ denotes average with respect to $\mathcal{P}_t$, while $\mathbb{E}[]$ denotes average with respect to the Brownian processes $\{B_t^j\}$.

As measurements occur independently on every site, we obtain the stochastic evolution of the monitored system as the sum of (1) and (4):

$$d\mathcal{P}_t = \mathcal{L}(\mathcal{P}_t)dt + \frac{\sqrt{\gamma}}{2}\sum_j \mathcal{P}_t(\vec{X})(X_j - \langle X_j\rangle_t)dB_t^j. \tag{5}$$

Note that, since $\mathcal{L}$ preserves the total probability and $\sum_{\{\vec{X}\}}\mathcal{P}_t(\vec{X})(X_j - \langle X_j\rangle_t) = 0$, the probability distribution $\mathcal{P}_t$ remains normalized at every time t for each realization of the process.

Single-particle problem We now consider the specific case of a single random walker. For lightness, the following discussion will be for a 1D system of N sites with periodic boundary conditions but generalization to higher dimensions is straightforward. Let $p_j(t)$ be the probability for the particle to be at site j at time t. We choose $\mathcal{L}$ to be the discrete Laplacian weighted by a diffusion constant D, i.e $\mathcal{L} = D\Delta$ with $\Delta p_j := p_{j-1} - 2p_j + p_{j+1}$. Starting from (5), the evolution of p_j in the presence of monitoring is given by

$$dp_j = D\Delta p_j dt + \sqrt{\gamma}p_j dW_t^j , \tag{6}$$

with $dW_t^j := dB_t^j - \sum_m p_m dB_t^m$ (see [41] for the details of the calculation). Note that dW_t^j are site-correlated Gaussian noises such that $\mathbb{E}[dW_t^j] = 0$ and $\mathbb{E}[dW_t^j dW_t^k] = (\delta_{j,k} - (p_j + p_k) + \sum_m p_m^2)dt$.

The diffusive term favors the flat, maximally entropic distribution $p_j = 1/N$ while the measurement term favors the N pointer states $p_j = \delta_{j,k}$ for fixed $k \in [\![1, N]\!]$. For finite D and γ, the stationary distribution of this model is non-trivial and, to the best of our knowledge, not known with a notable exception for $N = 2$. In the latter case, it turns out that the dynamics is equivalent to the one of a single qubit undergoing both thermal relaxation and quantum measurements and was treated in [42, 43].

Eq.(6) is reminiscent of the stochastic heat equation (SHE) with multiplicative noise [44] except that the noise dW_t^j is the sum of a Brownian process and a non-local contribution $\sum_m p_m dB_t^m$. Nonetheless, it turns out that there is a formal correspondence between (6) and the SHE in the regime of small γ.

Small γ regime To highlight this correspondence, we now perform a perturbative analysis around $\gamma = 0$ of (6) in the infinite system size limit $N \to \infty$. Suppose p admits the small γ expansion

$$p = p^{(0)} + \sqrt{\gamma}p^{(1)} + \gamma p^{(2)} + \cdots , \tag{7}$$

where $p^{(0)}$ is the stationary flat profile of the maximally entropic state, i.e $p_j^{(0)}(t) = 1/N, \forall(j, t)$. Inserting (7) into (6), we obtain the evolution of $p^{(1)}$ as

$$dp_j^{(1)} = D\Delta p_j^{(1)}dt + \frac{1}{N}(dB_t^j - \sum_m \frac{1}{N}dB_t^m). \tag{8}$$

The term $\sum_m \frac{dB_t^m}{N}$ has mean 0 and variance $1/N$ so it is subleading in the limit $N \to \infty$. In this regime, we get

$$dp_j^{(1)} \approx D\Delta p_j^{(1)} dt + p_j^{(0)} dB_t^j. \tag{9}$$

The evolution of $p^{(2)}$ is obtained in a similar way:

$$\begin{aligned} dp_j^{(2)} =& D\Delta p_j^{(2)} dt + \\ & p_j^{(1)}(dB_t^j - \underbrace{\sum_m \frac{1}{N} dB_t^m}_{:=\mathrm{I}}) \underbrace{- \frac{1}{N} \sum_m p_m^{(1)} dB_t^m}_{:=\mathrm{II}}. \end{aligned} \tag{10}$$

As explained above, the variance of I scales as $1/N$. The variance of II is given by $\mathbb{E}[\frac{1}{N^2}\sum_j (p_j^{(1)})^2]$. Using translational invariance, we have on the other hand that $\mathbb{E}[(p_j^{(1)})^2] = \mathbb{E}[\frac{1}{N}\sum_j (p_j^{(1)})^2]$ so there is a factor of N between the variance of the multiplicative noise term $p_j^{(1)} dB_t^j$ and II. Thus, in the limit of large N, we can neglect I and II to obtain

$$dp_j^{(2)} \approx D\Delta p_j^{(2)} dt + p_j^{(1)} dB_t^j. \tag{11}$$

This equation is structurally equivalent to Eq.(9). Thus, to order γ, the discrete SHE with multiplicative noise

$$dp_j = D\Delta p_j dt + \sqrt{\gamma} p_j dB_t^j \tag{12}$$

is a good approximation of (6). Furthermore, the probability p_j of the SHE is connected to the height h_j of the KPZ equation via the Cole-Hopf transformation [3] $h_j := \frac{1}{\sqrt{\gamma}} \log p_j$. Indeed, using standard Itō calculus on (12), we readily obtain the stochastic dynamics of h_j as a discretized version of the celebrated KPZ equation (up to a linear shift in time $h_j \to h_j + \sqrt{\gamma} t$):

$$dh_j = (D\Delta h_j + D\sqrt{\gamma}\,(\nabla h_j)^2 - \sqrt{\gamma}) dt + dB_t^j, \tag{13}$$

where ∇ is the discrete derivative $\nabla h_j := h_{j+1} - h_j$. Note that since $p_j \in [0,1]$, $h_j \in]-\infty, 0]$. Through its connection to the SHE, and therefore to the KPZ equation, we expect the dynamics of the monitored random walker to share common features with the physics of interface growth. One of the interesting quantities arising in the study of such interfaces is the so-called width w defined as

$$w := (\frac{1}{N}\sum_j (h_j - \bar{h})^2)^{1/2}, \tag{14}$$

where $\bar{h} := \frac{1}{N}\sum_j h_j$. Starting from a flat initial profile, the Family-Vicsek (F-V) scaling relation [1, 45] conjectures that, for scale-invariant interfaces, the width should behave as

$$w \propto N^{\alpha} f\left(\frac{t}{N^{\alpha/\beta}}\right) \tag{15}$$

with $f(u) \propto u^{\beta}$ for $u \ll 1$ and $f(u) \propto$ const for $u \gg 1$. The parameters α and β are respectively called the roughening and growth exponents. For models within the KPZ universality class, it has been shown in 1D [3] that $\alpha_{\mathrm{KPZ}}^{\mathrm{1D}} = 1/2$ and $\beta_{\mathrm{KPZ}}^{\mathrm{1D}} = 1/3$. We thus expect that the width of the log-probability of the monitored random walker will follow (15) with KPZ exponents when γ is small (see Fig.2-a and Fig.2-b).

Importantly, one can alternatively think of the small γ expansion as a short time limit. Indeed, at short times, $t \ll \gamma^{-1}$, the probability profile will be close to the initial flat distribution. If we assume that the leading term in p_j scales like $1/N$, it is easy to check that $\mathbb{E}[(\sum_m p_m dB_t^m)^2] \approx O(N^{-1})dt$ so that the contribution of the non-local part of dW_t^j is subleading.

However, in the long-time regime $t \gg \gamma^{-1}$, we expect to be pushed out of the KPZ regime as the roughening of the probability profile makes the non-local term of the noise grow.

In addition, the mapping to KPZ physics at short times and/or small γ tells us that a roughening phase transition from a smooth to a rough interface should occur in 3D and above [46–49]. Indeed, at small γ, we can neglect the contribution of the non-local part of the noise and thus the perturbative dynamic renormalization flow leads to similar flow equations than those of the KPZ equations [3]. In the smooth phase, the roughening term becomes irrelevant so we can safely neglect the non-local part of the noise. There, we expect that our model will flow to the same universality class as the KPZ equation, i.e the Edwards-Wilkinson (EW) class. However, this similarity should break down in the roughening phase where we expect (6) to flow to a different universality class than KPZ.

Although the analytical investigation of the strong γ regime is beyond the scope of this paper, we performed a series of numerical simulations of (6) in 1D and 3D to confirm the previous qualitative reasoning regarding the renormalization flow.

Numerical results We started all our simulations with a flat initial profile $p_j(t=0) = 1/N^d$, i.e $h_j(t=0) = -\frac{d}{\sqrt{\gamma}} \log N$ with d being the dimension. We simulated (6) using a standard Euler-Maruyama scheme and took the logarithm for every single realization to obtain the evolution of the process h_j. Details about the numerical methods, convergence check and finite-size scaling are provided in the SM [41].

We plot on Fig.1-a the rescaled width $\hat{w} = w/N^{\alpha_{\mathrm{M}}^{\mathrm{1D}}}$ as a function of the rescaled time $\hat{t} = t/N^{\alpha_{\mathrm{M}}^{\mathrm{1D}}/\beta_{\mathrm{KPZ}}^{\mathrm{1D}}}$ in 1D for different system sizes when $\gamma = 4.0$. In agreement with the connection to KPZ at short times, all curves collapse on the power law $t^{\beta_{\mathrm{KPZ}}^{\mathrm{1D}}}$ at small $\hat{t}$. However, beyond this regime, the F-V scaling of the width flows to a new universality class characterized by $\beta_{\mathrm{M}}^{\mathrm{1D}} \approx 1.4$ and $\alpha_{\mathrm{M}}^{\mathrm{1D}} \approx 1$.

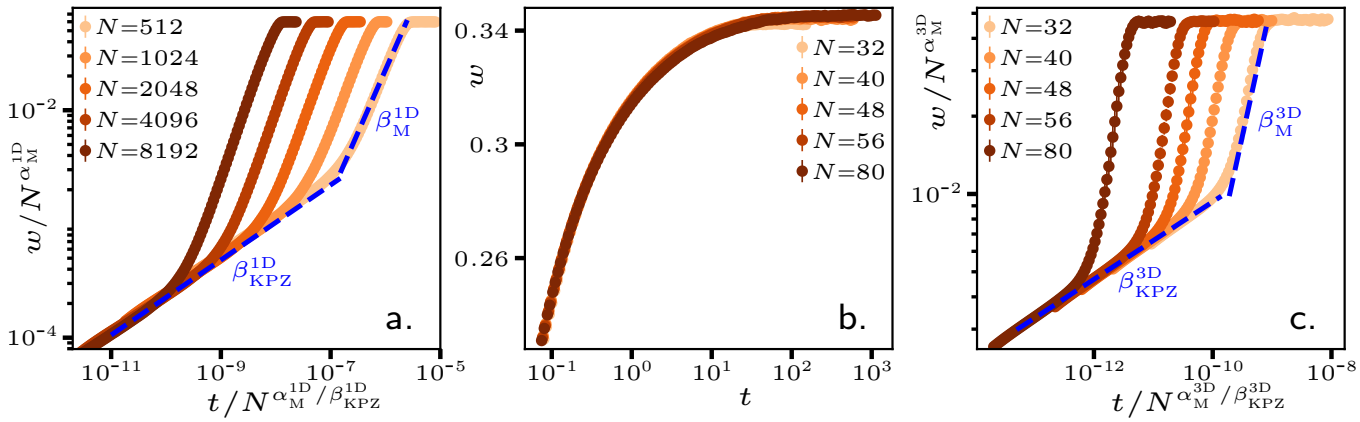


FIG. 1. **(a)**: Log-Log plot of the rescaled width $w/N^{\alpha_{\rm M}^{\rm 1D}}$ as a function of the rescaled time $t/N^{\alpha_{\rm M}^{\rm 1D}/\beta_{\rm KPZ}^{\rm 1D}}$ for a measurement rate $\gamma = 4$ in 1D. Exponents: $\alpha_{\rm M}^{\rm 1D} = 1$ and $\beta_{\rm KPZ}^{\rm 1D} = 0.34$. **Parameters**: $D = 1$, $dt = 0.001$. **(c)**: Log-Log plot of the rescaled width $w/N^{\alpha_{\rm M}^{\rm 3D}}$ as a function of the rescaled time $t/N^{\alpha_{\rm M}^{\rm 3D}/\beta_{\rm KPZ}^{\rm 3D}}$ for a measurement rate $\gamma = 36$ in 3D. Exponents: $\alpha_{\rm M}^{\rm 3D} = 1$ and $\beta_{\rm KPZ}^{\rm 3D} = 0.15$. **Parameters**: $D = 1$, $dt = 0.0002$. **(a) and (c)**: In accordance with the perturbative analysis, which is valid at short times, the initial growth exponent is always KPZ-like. At intermediate and large $\hat{t}$ however, the F-V scaling of the width flows to a new universality class characterized by $\beta_{\rm M}^{\rm 1D} \simeq 1.4$ and $\alpha_{\rm M}^{\rm 1D} \approx 1$ in 1D or $\beta_{\rm M}^{\rm 3D} \simeq 1.2$ and $\alpha_{\rm M}^{\rm 3D} \approx 1$ in 3D. **(b)**: Linear-Log plot of the width w as a function of time t for a measurement rate $\gamma = 4$ in 3D. As $\gamma < \gamma_{\rm M}^c$, the system is in the smooth EW phase and the width do not show any dependency on the system size. **Parameters**: $D = 1$, $dt = 0.002$.

Fig.1-c is a similar plot but performed in 3D when $\gamma = 36$ and for which the rescaled width and time are respectively given by $\hat{w} = w/N^{\alpha_{\rm M}^{\rm 3D}}$ and $\hat{t} = t/N^{\alpha_{\rm M}^{\rm 3D}/\beta_{\rm KPZ}^{\rm 3D}}$. At small $\hat{t}$, all curves collapse on the expected power law $t^{\beta_{\rm KPZ}^{\rm 3D}}$ while beyond this regime the F-V scaling flows to a new universality class characterized by $\beta_{\rm M}^{\rm 3D} \approx 1.2$ and $\alpha_{\rm M}^{\rm 3D} \approx 1$.

Finally, on Fig.1-b, we plot w as a function of t in 3D for different system sizes when $\gamma = 4$. For this value of γ, the KPZ equation flows toward the smooth EW class where we expect the non-local part of the noise to be irrelevant. In agreement with this intuition, Fig.1-b shows indeed that the width does not scale with N.

We report on Fig.2 the critical exponents as a function of γ for simulations performed on 1D and 3D lattices. For the former case (Fig.2-a and Fig.2-b), we observe a size-dependent crossover between the KPZ phase and a new phase characterized by exponents $\alpha_{\rm M}^{\rm 1D} \approx 1$ and $\beta_{\rm M}^{\rm 1D} \approx 1.4$. For the 3D case, we report on Fig.2-c the existence of a finite range over which $\alpha_{\rm M}^{\rm 3D}$ is close to 0, thereby indicating the presence of two distinct phases separated by a critical value $\gamma_{\rm M}^c \approx 10$. For comparison, 2-d shows the behavior of $\alpha_{\rm KPZ}^{\rm 3D}$ with respect to γ when simulating the SHE equation (12) in 3D where we find $\gamma_{\rm KPZ}^c \approx 10$. The fact that the two critical values for the SHE and our model are close corroborate our previous qualitative reasoning concerning the smooth phase in 3D. As we are only interested in the existence of a MIPT, we only reported the behavior of $\alpha_{\rm M}^{\rm 3D}$ as the systematic determination of $\beta_{\rm M}^{\rm 3D}$ is more involved and left for future works.

Conclusion and perspectives In this paper we introduced and studied a model for a single random walker undergoing continuous measurement. In the regime of weak monitoring, we mapped the time evolution of its probability distribution onto the SHE. We deduced that, in this regime, the width of the log probability follows the F-V scaling relation of the KPZ universality class. In 1D, this corresponds to roughening and growth exponents $\alpha_{\rm KPZ}^{\rm 1D} = 1/2$ and $\beta_{\rm KPZ}^{\rm 1D} = 1/3$. Beyond weak monitoring, we numerically find in 1D that increasing γ leads to a crossover from the KPZ class to a new universality class with exponents $\alpha_{\rm M}^{\rm 1D} \approx 1$ and $\beta_{\rm M}^{\rm 1D} \approx 1.4$. In 3D, we showed, again numerically, that this crossover becomes a phase transition between a smooth phase that we identify as the EW class and a new phase with $\alpha_{\rm M}^{\rm 3D} \approx 1$.

Our study is one of the first characterization of a MIPT in classically monitored systems and opens the door to several interesting questions. It would be most desirable to have a better analytical characterization of the strong γ regime. Since perturbative methods ought to fail there, non-perturbative RG methods such as the one presented in [49] may be employed there.

While we only considered a flat profile, it is known that different initial distributions leads to different universality classes in KPZ physics [4]. Thus, it would be interesting to investigate various initial states such as wedge or Brownian conditions to assess the effect of continuous monitoring on their corresponding exponents.

Finally, while we only studied a single particle, the continuous measurement process (5) is easily generalized to more intricate, many-body interacting problems. A natural extension would be to consider the symmetric simple exclusion process (SSEP), which describes multiple diffusive particle with hard-core

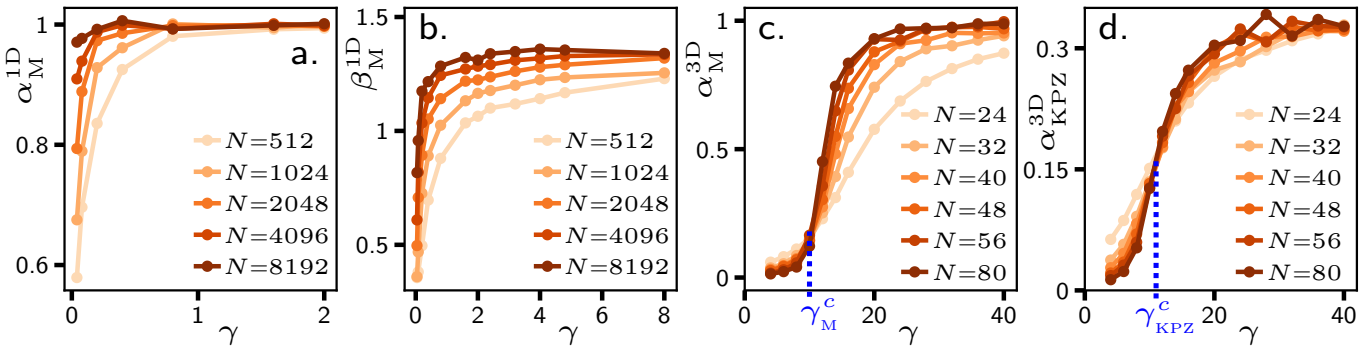


FIG. 2. **(a)**: Roughening exponent $\alpha_{\rm M}^{\rm 1D}$ as a function of γ for different system sizes. **(b)**: Second growth exponent $\beta_{\rm M}^{\rm 1D}$ as a function of γ for different system sizes. **(c)**: Roughening exponent $\alpha_{\rm M}^{\rm 3D}$ as a function of γ for different system sizes. **(d)**: Roughening exponent $\alpha_{\rm KPZ}^{\rm 3D}$ as a function of γ for different system sizes. Details about the methods used to extract the α's and β's are in the SM [41]. Note that, due to numerical limitations, only the roughening exponent was computed for the 3D case. The 1D case **(a)**-**(b)** shows a size-dependent crossover from the KPZ exponents $\alpha_{\rm KPZ}^{\rm 1D} = 1/2$, $\beta_{\rm KPZ}^{\rm 1D} = 1/3$ to a new phase with exponents $\alpha_{\rm M}^{\rm 1D} \approx 1$, $\beta_{\rm M}^{\rm 1D} \approx 1.4$. For the 3D case **(c)**, we observe that $\alpha_{\rm M}^{\rm 3D}$ remains constant close to 0 on a finite interval before jumping to $\alpha_{\rm M}^{\rm 3D} \approx 1$ when γ is greater than a critical value $\gamma_{\rm M}^{c} \approx 10$. This step-like behavior indicates a phase transition from the EW class to a new universality class in 3D. For comparison, **(d)** shows the behavior of $\alpha_{\rm KPZ}^{\rm 3D}$ as a function of γ for the standard SHE (12) in 3D where we also find $\gamma_{\rm KPZ}^{c} \approx 10$.

repulsion. Interestingly the SSEP can be promoted to a quantum version called the QSSEP [50, 51]. The study of both SSEP and QSSEP would thus provide a unified framework to disentangle the properties specific to quantum and classical systems under continuous monitoring.

Acknowledgements T.J and D.M thanks D. Bernard, N. Caballero, L. Canet, A. Krajenbrink, V. Lecomte, P. Ledoussal, M. Medenjak, C. Nardini and L. Piroli for useful discussions. We are grateful to Y. Sato for his game TimeBomb© which served as an inspiration for this work. T.J acknowledges support from the Swiss National Science Foundation under Division II. *During the writing of the manuscript, it came to our knowledge that two works with a similar objective of studying measurement effects on chaotic, classical systems but with a focus on phase transition were put as preprints [52, 53]*

* zizhuo.jin@unige.ch
† dgmartin@uchicago.edu

[1] A.-L. Barabási and H. E. Stanley, *Fractal Concepts in Surface Growth* (Cambridge University Press, 1995).
[2] G. Ódor, Rev. Mod. Phys. **76**, 663 (2004).
[3] M. Kardar, G. Parisi, and Y.-C. Zhang, Phys. Rev. Lett. **56**, 889 (1986).
[4] I. Corwin, arXiv e-prints , arXiv:1106.1596 (2011), arXiv:1106.1596 [math.PR].
[5] P. Meakin, P. Ramanlal, L. M. Sander, and R. C. Ball, Phys. Rev. A **34**, 5091 (1986).
[6] E. Murray, in *Proceedings of the Fourth Berkeley Symposium on Mathematical Statistics and Probability: Held at the Statistical Laboratory, University of California, June 20-July 30, 1960*, Vol. 2 (Univ of California Press, 1960) p. 223.
[7] M. Kolb, R. Botet, and R. Jullien, Phys. Rev. Lett. **51**, 1123 (1983).
[8] J. M. Kim and J. M. Kosterlitz, Phys. Rev. Lett. **62**, 2289 (1989).
[9] A. Nahum, J. Ruhman, S. Vijay, and J. Haah, Phys. Rev. X **7**, 031016 (2017).
[10] D. Bernard and P. L. Doussal, EPL (Europhysics Letters) **131**, 10007 (2020).
[11] T. Jin, A. Krajenbrink, and D. Bernard, Phys. Rev. Lett. **125**, 040603 (2020).
[12] C. Zu, F. Machado, B. Ye, S. Choi, B. Kobrin, T. Mittiga, S. Hsieh, P. Bhattacharyya, M. Markham, D. Twitchen, A. Jarmola, D. Budker, C. R. Laumann, J. E. Moore, and N. Y. Yao, Nature **597**, 45 (2021).
[13] J. De Nardis, M. Medenjak, C. Karrasch, and E. Ilievski, Phys. Rev. Lett. **124**, 210605 (2020).
[14] E. Ilievski, J. De Nardis, S. Gopalakrishnan, R. Vasseur, and B. Ware, Phys. Rev. X **11**, 031023 (2021).
[15] D. Wei, A. Rubio-Abadal, B. Ye, F. Machado, J. Kemp, K. Srakaew, S. Hollerith, J. Rui, S. Gopalakrishnan, N. Y. Yao, I. Bloch, and J. Zeiher, arXiv e-prints , arXiv:2107.00038 (2021), arXiv:2107.00038 [cond-mat.quant-gas].
[16] Q. Fontaine, D. Squizzato, F. Baboux, I. Amelio, A. Lemaître, M. Morassi, I. Sagnes, L. Le Gratiet, A. Harouri, M. Wouters, I. Carusotto, A. Amo, M. Richard, A. Minguzzi, L. Canet, S. Ravets, and J. Bloch, arXiv e-prints , arXiv:2112.09550 (2021), arXiv:2112.09550 [cond-mat.mes-hall].
[17] Y. Aharonov, D. Z. Albert, and L. Vaidman, Phys. Rev. Lett. **60**, 1351 (1988).
[18] J. M. Raimond, M. Brune, and S. Haroche, Rev. Mod. Phys. **73**, 565 (2001).
[19] W. M. Itano, D. J. Heinzen, J. J. Bollinger, and D. J. Wineland, Phys. Rev. A **41**, 2295 (1990).
[20] S. Kocsis, B. Braverman, S. Ravets, M. J. Stevens, R. P. Mirin, L. K. Shalm, and

A. M. Steinberg, Science **332**, 1170 (2011), https://www.science.org/doi/pdf/10.1126/science.1202218.
[21] N. Cottet, S. Jezouin, L. Bretheau, P. Campagne-Ibarcq, Q. Ficheux, J. Anders, A. Auffèves, R. Azouit, P. Rouchon, and B. Huard, Proceedings of the National Academy of Sciences **114**, 7561 (2017), https://www.pnas.org/doi/pdf/10.1073/pnas.1704827114.
[22] Z. K. Minev, S. O. Mundhada, S. Shankar, P. Reinhold, R. Gutiérrez-Jáuregui, R. J. Schoelkopf, M. Mirrahimi, H. J. Carmichael, and M. H. Devoret, Nature **570**, 200 (2019).
[23] X. Cao, A. Tilloy, and A. De Luca, SciPost Physics **7**, 024 (2019).
[24] B. Skinner, J. Ruhman, and A. Nahum, Phys. Rev. X **9**, 031009 (2019).
[25] Y. Li, X. Chen, and M. P. A. Fisher, Phys. Rev. B **100**, 134306 (2019).
[26] M. Szyniszewski, A. Romito, and H. Schomerus, Phys. Rev. B **100**, 064204 (2019).
[27] Y. Bao, S. Choi, and E. Altman, Phys. Rev. B **101**, 104301 (2020).
[28] M. J. Gullans and D. A. Huse, Phys. Rev. Lett. **125**, 070606 (2020).
[29] M. J. Gullans and D. A. Huse, Phys. Rev. X **10**, 041020 (2020).
[30] A. Zabalo, M. J. Gullans, J. H. Wilson, S. Gopalakrishnan, D. A. Huse, and J. H. Pixley, Phys. Rev. B **101**, 060301 (2020).
[31] A. Lavasani, Y. Alavirad, and M. Barkeshli, Nature Physics **17**, 342 (2021).
[32] M. Buchhold, Y. Minoguchi, A. Altland, and S. Diehl, Phys. Rev. X **11**, 041004 (2021).
[33] X. Turkeshi, A. Biella, R. Fazio, M. Dalmonte, and M. Schiró, Phys. Rev. B **103**, 224210 (2021).
[34] P. Sierant and X. Turkeshi, Phys. Rev. Lett. **128**, 130605 (2022).
[35] Z. Weinstein, Y. Bao, and E. Altman, Measurement-induced power law negativity in an open monitored quantum circuit (2022).
[36] J. Dalibard, Y. Castin, and K. Mølmer, Phys. Rev. Lett. **68**, 580 (1992).
[37] K. Jacobs and D. A. Steck, Contemporary Physics **47**, 279 (2006), https://doi.org/10.1080/00107510601101934.
[38] M. Bauer, D. Bernard, and A. Tilloy, Journal of Statistical Mechanics: Theory and Experiment **2014**, P09001 (2014).
[39] D. Bernard, T. Jin, and O. Shpielberg, EPL (Europhysics Letters) **121**, 60006 (2018).
[40] L. Rabiner and B. Juang, IEEE ASSP Magazine **3**, 4 (1986).
[41] Supplementary material.
[42] M. Bauer and D. Bernard, Letters in Mathematical Physics **104**, 707 (2014).
[43] A. Tilloy, M. Bauer, and D. Bernard, Phys. Rev. A **92**, 052111 (2015).
[44] L. Bertini and N. Cancrini, Journal of Statistical Physics **78**, 1377 (1995).
[45] F. Family and T. Vicsek, Journal of Physics A: Mathematical and General **18**, L75 (1985).
[46] K. Moser, J. Kertész, and D. E. Wolf, Physica A: Statistical Mechanics and its Applications **178**, 215 (1991).
[47] H. Yan, D. Kessler, and L. M. Sander, Phys. Rev. Lett. **64**, 926 (1990).
[48] M. F. Torres and R. C. Buceta, Journal of Statistical Mechanics: Theory and Experiment **2018**, 033208 (2018).
[49] L. Canet, H. Chaté, B. Delamotte, and N. Wschebor, Phys. Rev. Lett. **104**, 150601 (2010).
[50] M. Bauer, D. Bernard, and T. Jin, SciPost Phys. **6**, 45 (2019).
[51] D. Bernard and T. Jin, Phys. Rev. Lett. **123**, 080601 (2019).
[52] J. Willsher, S.-W. Liu, R. Moessner, and J. Knolle, Measurement-induced phase transition in a classical, chaotic many-body system (2022).
[53] A. Pizzi, D. Malz, A. Nunnenkamp, and J. Knolle, Bridging the gap between classical and quantum many-body information dynamics (2022).
[54] R. Mannella, arXiv preprint cond-mat/9709326 (1997).
[55] F. Moss and P. V. E. McClintock, eds., *Experiments and simulations*, Noise in nonlinear dynamical systems No. v. 3 (Cambridge University Press, Cambridge [Cambridgeshire] ; New York, 1989).

SUPPLEMENTARY MATERIAL

1. Derivation of the model

In this supplementary material, we present the derivation of (5) and (6) of the main text.

The state of system is described by a set of random variables $\{X_1, \cdots, X_N\} := \vec{X}$ which can take values ± 1 where $+1$ corresponds to an occupied site and -1 to an empty site. The ancilla monitoring site j is also described by a random variable A_j which can take binary values $\{-1, 1\}$. We denote by $\mathcal{P}(\vec{X}, A_j)$ the joint probability of the union system+ancilla to be in a given configuration. We fix this probability distribution to

$$\mathcal{P}(\vec{X}, A_j) = \mathcal{P}(\vec{X}) \frac{1 + \varepsilon A_j X_j}{2} \ , \tag{16}$$

with $\varepsilon = \frac{\sqrt{\gamma \delta t}}{2}$ being a small paramater and $\mathcal{P}(\vec{X})$ being the reduced probability of the system only. The joint distribution (16) implies that the state of ancilla j and its corresponding site are positively correlated: if $A_j = 1$, it's more likely to find X_j in state 1. The reduced probability $\mathcal{P}(A_j)$ for the j-th ancilla is given by

$$\mathcal{P}(A_j) = \sum_{\{\vec{X}\}} \mathcal{P}(\vec{X}, A_j) = \frac{1}{2}(1 + \varepsilon A_j \langle X_j \rangle). \tag{17}$$

Once a measurement of the state of the ancilla has been made with outcome A_j, the probability distribution is updated with probability $\mathcal{P}(A_j)$ to

$$\mathcal{P}(\vec{X}) \to \mathcal{P}(\vec{X}|A_j) = \mathcal{P}(\vec{X}) \frac{1 + \varepsilon A_j X_j}{1 + \varepsilon A_j \langle X_j \rangle} \ , \tag{18}$$

which is just Bayes law. We now repeat this procedure M times with a fresh ancilla $A_j^{(n)}$ indexed by $n \in [\![1, M]\!]$. Expanding (18) to order ε^2, we get:

$$\mathcal{P}_{n+1}(\vec{X}|A_j^{(n)}) = \mathcal{P}_n(\vec{X}) \left(1 + \varepsilon A_j^{(n)} X_j\right) \left(1 - \varepsilon A_j^{(n)} \langle X_j \rangle_n + \varepsilon^2 \left(A_j^{(n)} \langle X_j \rangle_n\right)^2\right) + O(\varepsilon^3) \tag{19}$$

$$= \mathcal{P}_n(\vec{X}) \left(1 + \varepsilon A_j^{(n)} \left(X_j - \langle X_j \rangle_n\right) - \varepsilon^2 \left(X_j \langle X_j \rangle_n - \langle X_j \rangle_n^2\right)\right) + O(\varepsilon^3) \ , \tag{20}$$

where $\langle \rangle_n$ indicates that the average has to be taken with $\mathcal{P}_n$ and we used that $(A_j^{(n)})^2 = 1$. The signal is defined as the sum of the measurement outputs on the ancilla, i.e $S_{j,M} := \sum_{n=1}^{M} \varepsilon A_j^{(n)}$, from which we deduce its increment $S_{j,M+1} - S_{j,M} = \varepsilon A_j^{(M+1)}$. Using (17), we further obtain that

$$\langle \varepsilon A_j^{(n)} \rangle = \frac{\varepsilon}{2}(1 + \varepsilon \langle X_j \rangle_n) - \frac{\varepsilon}{2}(1 - \varepsilon \langle X_j \rangle_n) = \varepsilon^2 \langle X_j \rangle_n \ , \qquad \langle (\varepsilon A_j^{(n)})^2 \rangle = \varepsilon^2 \ . \tag{21}$$

These relations show that in the limit $\varepsilon \to 0$, $M\delta t = t$, the signal converges in law towards a process described by the following stochastic differential equation

$$dS_{j,t} = \frac{\gamma}{4} \langle X_j \rangle_t dt + \frac{\sqrt{\gamma}}{2} dB_t^j \ , \tag{22}$$

where j is the site index and B_t^j is a 0-mean, site-independent Brownian process of variance $\mathbb{E}[B_t^j B_t^i] = \delta_{ij} dt$. We can now replace the A_j's in the evolution equation for the probability (20) to get

$$d\mathcal{P}_t(\vec{X}) = \mathcal{P}_t(\vec{X}) \left(\left(\frac{\gamma}{4} \langle X_j \rangle_t dt + \frac{\sqrt{\gamma}}{2} dB_t^j \right) \left(X_j - \langle X_j \rangle_t\right) - \frac{\gamma}{4} \left(X_j \langle X_j \rangle_t - \langle X_j \rangle_t^2\right) dt \right) = \frac{\sqrt{\gamma}}{2} \mathcal{P}_t(\vec{X}) \left(X_j - \langle X_j \rangle_t\right) dB_t^j . \tag{23}$$

If measurement processes occur independently on every site and we include the internal stochastic dynamics $\mathcal{L}$ of the system, we obtain the following SDE for $\mathcal{P}_t$:

$$d\mathcal{P}_t = \mathcal{L}(\mathcal{P}_t) dt + \frac{\sqrt{\gamma}}{2} \sum_j \mathcal{P}_t(\vec{X}) (X_j - \langle X_j \rangle_t) dB_t^j \ , \tag{24}$$

which is (5) in the main text.

We now specify to the particular case of a single random walker on a discrete lattice of N sites with periodic boundary conditions. In this case, we define $p_j(t) := \mathcal{P}_t(X_1 = -1, \cdots, X_j = 1, \cdots, X_N = -1)$ and we further have that

$$\mathcal{L}(p_j) = D(p_{j-1} - 2p_j + p_{j+1}), \qquad \langle X_j \rangle_t = \sum_{j' \neq j} -p_{j'} + p_j = -1 + 2p_j \ . \tag{25}$$

Inserting (25) into (24), we obtain the time-evolution of p_j (Eq.(6) in main text) as

$$\begin{aligned} dp_j &= D(p_{j-1} - 2p_j + p_{j+1}) + \frac{\sqrt{\gamma}}{2} \left(\sum_{m \neq j} p_m(-2p_j) dB_t^m + p_j(2 - 2p_j) dB_t^j \right), \\ &= D(p_{j-1} - 2p_j + p_{j+1}) + \sqrt{\gamma} p_j \left(dB_t^j - \sum_m p_m dB_t^m \right) \ . \end{aligned} \tag{26}$$

2. Numerical methods

We hereafter describe the methods employed to numerically integrate (6). We first note the peculiar structure of the noise term dW_t^j in (6): it is a multiplicative multi-dimensional noise. Thus, (6) falls into the class of stochastic differential equations taking the form

$$\frac{dx_j}{dt} = f_j(\{\mathbf{x}\}) + \sum_{i=1}^{N} g_{ji}(\{\mathbf{x}\}) \xi_i \tag{27}$$

where ξ_i's are gaussian white noises such that $\langle \xi_i(s) \xi_k(s') \rangle = \delta_{ik} \delta(s - s')$, and f_j and g_{ji} are functions of the set of position $\{\mathbf{x}\} = \{x_k, \ k \in [1, .., N]\}$. Numerical integration schemes for SDEs of type (27) have been discussed in [54] and chapter 7 of [55]. The combination of the multiplicative and multi-dimensional nature of the noise in (27) renders usual higher order Runge-Kutta-based SDE algorithms inoperative. As described in [55], the two numerical schemes available for integrating (27) are both of order dt at maximum. The first one is an Euler-Maruyama scheme, (ie simple forward Euler), which allows for a straightforward integration of (27) in Ito prescription. The second one is a first order Runge-Kutta scheme with an approximate closure valid up to dt: it allows for numerical integration of (27) directly in Stratonovitch prescription. As we studied (6) and within Ito formalism in the main text, we naturally choose the former Euler-Maruyama algorithm to perform our numerical integrations. To check the convergence of the algorithm, we divided the time step dt by two and verified the stability of our results (see Fig 3). We further constantly monitored the probabilities p_j's and choose a sufficiently low time step dt ensuring that $p_j(t) > 0$ for all $j \in [1, .., N]$ at every time t. Finally, we also monitored the conservation of probabilities and checked that $\sum_j p_j(t) = 1$ at every time t.

The width w at fixed γ and fixed system size N was obtained by averaging over at least 1000 realizations of (6). We made sure that simulations ran long enough for w to effectively reach its plateau value at large time. To compute the roughening exponent α at fixed γ, we performed a linear fit of the width's plateau value $w(t = \infty)$ as a function of the system size N in Log-Log. From (15), we indeed have that $\log(w(t = \infty)) \sim \alpha \log(N)$: the coefficient of the later linear fit gives α.

To extract the growth exponent β_{KPZ}, we performed a linear fit of the width w against t in Log-Log at small times. From our small-γ perturbative analysis and (15), we have that $\log(w(t)) \sim \beta_{\mathrm{KPZ}} \log(t)$ at small times and the coefficient of the later linear fit thus gives β_{KPZ}. In practise, we made sure to apply the linear fit only for small times where the logarithm of the width increases linearly with respect to t. Finally, to extract the second growth exponent β_{M}, we performed a linear fit of the width w against t in Log-Log at intermediate times. We made sure to perform the later fit in between the initial KPZ-like growth regime characterized by β_{KPZ} and the plateau regime characterized by α_{M}.

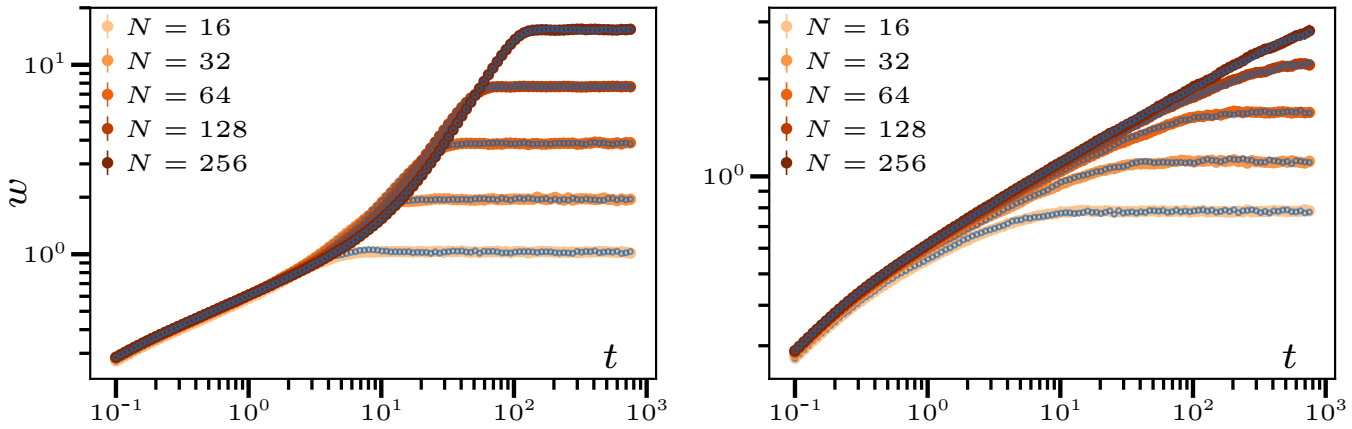


FIG. 3. **Left:** Width as a function of time for $dt = 0.001$ (orange shaded dots) and for $dt = 0.0005$ (unfilled blue circles) at different values of N and fixed $\gamma = 4$. **Right:** Same plot at fixed $\gamma = 0.02$. In both cases, the numerical algorithm has converged to the solution. **Parameters:** $D = 1$. To obtain the width w, we averaged over at least 1000 realizations of (6) such that the error bars of w (corresponding to its standard deviation) are too small to be noticed on the plots.